

The pertinent results are summarized in Table 1 where

$$\|\Delta\theta_q^*\| \triangleq \sum_i |\theta_q^*(s_i) - \theta_{q-1}^*(s_i)|$$

$$\|\Delta J_q^*\| \triangleq |(J_q^*)^{1/q} - (J_{q-1})^{1/q-1}|$$

and the s_i represent 126 equispaced points along the flight path. Univac 1108 computer run time to $q = 12$ and $q = 22$ was 4.43 and 9.27 minutes, respectively. It is interesting to note that after the first six passes the maximum flight path angle had been reduced from 1.49 rad (86°) to 1.18 rad (68°) but an additional five passes resulted in a further reduction of only 0.02 rad. Moreover, although there exists a significant difference between $\theta_{12}^*(s)$ and $\theta_{22}^*(s)$ for smaller s , as s approaches that point at which $\max |\gamma(t)|$ occurs θ_{12}^* and θ_{22}^* become nearly identical. A similar statement can be made for γ_{12}^* and γ_{22}^* . This behavior is due to the fact that the Chebycheff optimality criterion concerns itself only with the maximum of a time function and ignores other values of that function. These results tend to substantiate an observation made by Johnson² concerning the non-uniqueness of Chebycheff optimal controllers.

IV. Comments and Conclusions

A principal advantage of the Chebycheff algorithm presented here stems from the fact that the Chebycheff solution is obtained by solving a sequence of standard Bolza problems for which well-known analytic and computational techniques are available. Thus, results obtained over the past decade concerning the relative merits of first- and second-order search techniques, state and control variable constraints, etc., can be utilized in the Chebycheff algorithm. On the other hand, certain inherent limitations must be considered. In particular, the curves presented in Fig. 2 and the possibility of a nonunique optimal controller point to the desirability of using a norm on performance as a stopping criterion rather than a norm on control. However, in some problems J_q^* may exceed computer numeric limits for large q before $\|\Delta J_q^*\|$ has reached a stopping criterion. In these cases it becomes necessary to replace J_q as given in Eq. (3) by

$$J_q[u] = \int_{t_0}^{t_f} [g(t)/\hat{g}]^q dt$$

where \hat{g} is a normalizing constant used to maintain J_q within reasonable limits and to increase the rate of convergence of u_q^* to u^* .

For the optimization problem presented in the previous section, a search technique based only on first-order variations was used to compute u_q^* for each q . In general, it is to be expected by reasons of continuity that u_q^* would not be vastly dissimilar to u_{q+1}^* . Since u_q^* is used to initiate the search for u_{q+1}^* it thus appears that utilization of a second-order algorithm could achieve savings in total computer run time as well as increased accuracy.

References

- Neustadt, L. C., "Minimum Effort Control Systems," *Journal of Society for Industrial and Applied Mathematics*, Vol. 1, No. 1, 1962, pp. 16-31.
- Johnson, C. D., "Optimal Control with Chebyshev Minimax Performance Index," *Joint Automatic Control Conference*, AIAA, New York, 1966, pp. 345-358.
- Taylor, A. E., *Introduction to Functional Analysis*, Wiley, New York, 1958, p. 91.
- Thrasher, G. J., "Optimal Programming for Aircraft Trajectories Utilizing a New Strategy for Handling Inequality Constraints," AIAA Paper 69-812, Los Angeles, 1969.
- Thrasher, G. J., "Application of the Augmented Min-H Strategy to the Problem of Minimum-Time Atmospheric Trajectories," UARL Rept. G-110137-5, Oct. 1968, United Aircraft Research Laboratories, East Hartford, Conn.
- Gottlieb, R. G., "Rapid Convergence to Optimum Solutions using a Min-H Strategy," *AIAA Journal*, Vol. 5, No. 2, Feb. 1967, pp. 322-329.

Influence of Film Thickness on the Calibration of Thin-Film-Gage Backing Materials

RONALD K. HANSON*

Cranfield Institute of Technology, England

THIN-FILM resistance thermometers are now standard transducers in shock tubes and other high-speed-flow devices where a measurement of the transient surface temperature can be processed to yield, for example, heat-transfer rates,^{1,2} thermal conductivities of gases,^{3,4} and thermal accommodation coefficients.^{5,6} In each of these experiments one needs to know the value of the property $(\rho c \lambda)^{1/2}$ for the film backing material where ρ , c , and λ are, respectively, the substrate density, specific heat and thermal conductivity. Experience has shown that this quantity should be determined dynamically over a time interval comparable with the test time of the temperature-measurement experiment, and a very convenient pulse-heating technique has been developed for this purpose.⁷ It is generally assumed, in obtaining $(\rho c \lambda)^{1/2}$ of the substrate with this method, that the heat conduction is one dimensional, the substrate behaves as a semi-infinite medium and the film thickness is negligible. For short times, however, this model breaks down owing to the finite heat capacity of the film, and this effect can be important if one wishes to calibrate the gage for short-duration experiments, or if the film thickness is great. (Of course the model also breaks down for large times when two- and three-dimensional effects come into play.) This Note presents a solution for the response of a finite-thickness gage during pulse heating and suggests a simple, approximate means of obtaining $(\rho c \lambda)^{1/2}$ from pulse-heating data when finite-thickness effects are important.

Typically in the experiment a step voltage is applied to a simple bridge circuit, with the thin-film gage forming one arm of the bridge, thus subjecting the gage to a known (constant) heating pulse. The resulting bridge out-of-balance voltage, which can be monitored on an oscilloscope, is thus equivalent to the gage temperature-time history. The experiment is generally performed with the gage exposed to air and then repeated with the gage immersed in a standard liquid. If one neglects the film thickness and assumes that the heat is liberated at the surface of the backing material, $(\rho c \lambda)^{1/2}$ for the backing material follows directly from a known value of $(\rho c \lambda)^{1/2}$ for the liquid and the ratio of the bridge output voltages for the two experiments at the same time after pulse initiation.⁷ In the present model we consider that heat is generated uniformly throughout an infinite film, of thickness δ , mounted on a semi-infinite expanse of backing material. The film is bounded on the opposite side by a semi-infinite expanse of gas or liquid. Denoting the film as region 1, the solid substrate as region 2, and the gas or liquid as region 3, the appropriate equations to solve for one-dimensional heat conduction are (for constant thermal properties)

$$\partial^2 T_1 / \partial x^2 - (1/\alpha_1) \partial T_1 / \partial t = -A/\lambda_1 \quad (1)$$

and

$$\partial^2 T_{2,3} / \partial x^2 - (1/\alpha_{2,3}) \partial T_{2,3} / \partial t = 0 \quad (2)$$

where T is the temperature, α is the thermal diffusivity ($\alpha = \lambda/\rho c$), and A is the heat-generation rate per unit volume. Anticipating the usual experimental arrangement we take A constant. The heat generation is assumed to begin at $t = 0$ and the film-substrate interface is taken at $x = 0$, with the

Received October 21, 1970.

* Presently an NRC Postdoctoral Fellow at NASA Ames Research Center, Moffett Field, Calif.

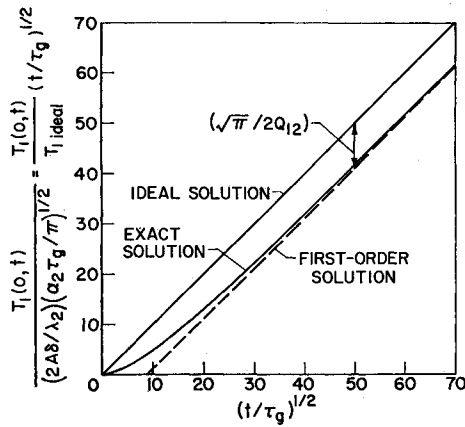


Fig. 1 Thin-film temperature response during pulse-heating calibration in air; $Q_{12} = 0.1$. The exact solution is based on Eq. (4); the ideal and first-order solutions are extracted from Eq. (5).

substrate occupying the half space $x > 0$ and the air or liquid interface located at $x = -\delta$. Without loss of generality we take the initial temperature to be everywhere zero. The boundary condition at infinity requires the temperature to remain unchanged. The boundary conditions at the film-substrate interface consist of matching the temperature and heat flux. Similar conditions are applied at the other film interface for the case of liquid in region 3, but for air in region 3 we assume that conduction between regions 1 and 3 is negligible so that $\partial T_1/\partial x = 0$ at $x = -\delta$. (In this latter case a diffusion equation for region 3 is not needed.) The temperature solution in region 1 is simply obtained using Laplace transform techniques⁸ together with the initial and boundary conditions mentioned previously.

Considering first the case with air in region 3, we find, for the transform of the temperature in region 1, after some algebra,

$$\bar{T}_1(x,s) = \frac{\alpha_1 A}{s^2 \lambda_1} \left(1 - \frac{Q_{12}}{1 + Q_{12}} \{ \exp[(s/\alpha_1)^{1/2} x] + \exp[-(s/\alpha_1)^{1/2} x - 2(s/\alpha_1)^{1/2} \delta] \} \sum_{n=0}^{\infty} \sigma^n \exp[-2n(s/\alpha_1)^{1/2} \delta] \right) \quad (3)$$

where $Q_{12} = [(\rho c \lambda)_2 / (\rho c \lambda)_1]^{1/2}$ and $\sigma = (1 - Q_{12}) / (1 + Q_{12}) < 1$.

Although the quantity of interest is the average temperature in region 1, the temperature gradients are small for the times of interest, so it suffices to take the inverse transform at a specific value of x . At $x = 0$ we find⁸

$$T_1(0,t) = [(\alpha_1 A t / \lambda_1)(1 + Q_{12})^{-1}] \times \left(1 - Q_{12}(1 + \sigma) \sum_{n=0}^{\infty} \sigma^n \{ [1 + 2(n+1)^2 \tau_g / t] \cdot \operatorname{erfc}[(n+1)(\tau_g/t)^{1/2}] - 2(n+1)(\tau_g/\pi t)^{1/2} \times \exp[-(n+1)^2 \tau_g / t] \} \right) \quad (4)$$

where τ_g is the characteristic diffusion time in the film, $\tau_g = \delta^2 / \alpha_1$. Equation (4) will be termed the exact solution for pulse heating in air. A useful approximate form of this result can be found by expanding the complementary error function and exponential terms for $(\tau_g/t)^{1/2} \ll 1$. Summing the expanded terms, one can show that, to first order,

$$T_1(0,t) = \frac{2A\delta}{\lambda_2} (\alpha_2 t / \pi)^{1/2} \left[1 - \frac{(\pi)^{1/2}}{2} \left(\frac{\tau_g}{t} \right)^{1/2} \frac{1}{Q_{12}} \right] \quad (5)$$

The term outside the brackets on the right-hand side of Eq. (5) is the *ideal* response of the substrate surface temperature for the case in which the same amount of heat is released directly at the substrate surface with no film present.⁸ The influence of the finite heat capacity of the film is exhibited by the first-order correction term inside the brackets. The ideal, exact and first-order solutions are all plotted, in dimensionless form, in Fig. 1. Because of the equivalence between the film temperature change and the bridge output voltage, the exact solution in Fig. 1 is effectively a record of the experimental pulse-heating response. The important observations to be made from Fig. 1 are that the exact solution asymptotes at large time to the first-order solution (rather than the ideal solution), and that the first-order solution differs from the ideal solution by a fixed amount.

If we choose platinum and pyrex as a typical film-substrate combination, then $Q_{12} \approx 0.1$, $\alpha_1 \approx 0.25 \text{ cm}^2/\text{sec}$, and the difference between the ideal and first-order solutions for the temperature is, at any time, approximately $18(\delta, \text{cm}) / (t, \text{sec})^{1/2}$. For a 2000 Å film, this difference amounts to about 36% at 1 μsec $[(t/\tau_g)^{1/2} \approx 26]$ and 3.6% at 100 μsec $[(t/\tau_g)^{1/2} \approx 260]$ after pulse initiation. For a gage 2 μ thick, the same decrements of 36% and 3.6% occur at times of 100 μsec and 10 msec, respectively. Since $(\rho c \lambda)^{1/2}$ calibrations are often carried out on the submillisecond time scale to avoid multidimensional effects, the effect of finite film thickness can obviously introduce a significant deviation from the ideal bridge output voltage. Fortunately, the exact solution is well approximated by the first-order solution for all but very short times, and we can use this information to account in a simple manner for thickness effects by fitting a straight line through the bridge response data plotted vs $(t)^{1/2}$. The slope of this line will correspond nearly to that of the first-order theoretical response (and hence also to the slope of the ideal response), the difference in slopes depending on the interval over which the bridge response data are plotted.

Turning now to a consideration of the pulse-heating experiment with the gage immersed in a liquid, we find that the film temperature solution is

$$T_1(0,t) = \frac{\alpha_1 A t}{\lambda_1(1 + Q_{12})} \left(1 - \frac{2Q_{12}}{1 - Q_{12}} \sum_{n=0}^{\infty} \beta^{n+1} \times \{ [1 + 2(n+1)^2 \tau_g / t] \operatorname{erfc}[(n+1)(\tau_g/t)^{1/2}] - 2(n+1)(\tau_g/\pi t)^{1/2} \exp[-(n+1)^2 \tau_g / t] \} - \frac{2Q_{13}}{1 + Q_{13}} \sum_{n=0}^{\infty} \beta^n \{ [1 + (2n+1)^2 \tau_g / 2t] \times \operatorname{erfc}[(2n+1)(\tau_g/4t)^{1/2}] - (2n+1)(\tau_g/\pi t)^{1/2} \times \exp[-(2n+1)^2 \tau_g / 4t] \} \right) \quad (6)$$

where $\beta = (1 - Q_{12})(1 - Q_{13}) / [(1 + Q_{12})(1 + Q_{13})] < 1$.

The approximate form of this result, for $(\tau_g/t)^{1/2} \ll 1$, is, to first order,

$$T_1(0,t) = \frac{2A\delta}{\lambda_2} \frac{(\alpha_2 t / \pi)^{1/2}}{1 + Q_{23}} \left[1 - \frac{(\pi)^{1/2}}{2} \left(\frac{\tau_g}{t} \right)^{1/2} \frac{B}{Q_{12} + Q_{13}} \right] \quad (7)$$

where

$$B = \frac{1}{1 - \beta} [(1 - Q_{13})Q_{12}(1 + \beta) + (Q_{13}/4)(1 + Q_{12})(1 + Q_{13})(1 + 6\beta + \beta^2)] \quad (8)$$

B may be set equal to 1 for values of Q_{12} and Q_{13} much less than 1, which is the case for the metal films, dielectric substrates and standard liquids of interest here. We thus recover the ideal solution for the deposition of heat at the interface of two semi-infinite materials⁸ modified by the correction factor in brackets. Again we see that the exact solution asymptotes to the first-order solution, and that the first-order solution

falls below the ideal result by a constant amount. Note that the correction term is smaller than that shown in the bracketed term of Eq. (5), however, because of the addition of Q_{13} to account for heat conducted into region 3.

An inspection of Eqs. (5) and (7) shows that film thickness effects are truly negligible only when $(t/\tau_0)^{1/2} \gg 1/Q_{12}$. In that instance alone Q_{23} , the ratio of thermal properties in the standard liquid and the backing material, follows directly from a ratio of the bridge output signals. If it is desirable or necessary to measure $(\rho c \lambda)^{1/2}$ of the substrate on a shorter time scale, finite film thickness must be accounted for, and this can be done to first order simply by comparing the slopes of straight lines fitted to bridge output records plotted vs $t^{1/2}$. The ratio of these slopes corresponds nearly to that of the theoretical first-order solutions and hence gives $1 + Q_{23}$ directly. [For analyses at time $(t/\tau_0)^{1/2} \lesssim 30$ the exact solution should be employed of course.] It is worth noting that, in view of the practical difficulty of obtaining a suitably accurate bridge balance prior to pulsing, it is good practice to use the slope technique even when film thickness effects are truly negligible.

The theory presented here was developed to complement a study of thermal accommodation processes utilizing the transient response of thin-film gages during a period of a few microseconds following exposure to a suddenly heated gas.⁶ It was thus desirable to measure $(\rho c \lambda)^{1/2}$ of the film substrate over a comparable period accounting for the possible influence of film thickness effects. Accordingly, several pulse-heating experiments were conducted using five different chemically deposited and vacuum-evaporated platinum gages. The films, which varied in thickness from 400–2000 Å,† were all mounted on pyrex. The bridge circuit was carefully designed to minimize initial electrical transients during the pulsing process; a very sensitive bridge-balancing procedure was used. The bridge output signal for each experiment was monitored for either a 10 μ sec or a 200 μ sec period following pulse initiation. All the short- and long-duration records, when coupled with the present theoretical model, produced $(\rho c \lambda)^{1/2}$ values for pyrex of 3.60×10^{-2} cal-cm⁻²°K⁻¹ sec^{-1/2} (at 25°C), with a maximum deviation of $\pm 0.13 \times 10^{-2}$. (The largest deviations occurred with the 10 μ sec duration records.) Both silicone fluid (type MS 200/100 cs)‡ and glycerine were used as standard liquids, with the silicone fluid tests producing somewhat less scatter. Values for $(\rho c \lambda)^{1/2}$ of the liquids were computed from handbooks and manufacturer's literature. The value of $(\rho c \lambda)^{1/2}$ inferred for pyrex in this work is in excellent agreement with previous measurements⁷ employing much longer time scales; so we may conclude that a) the value of $(\rho c \lambda)^{1/2}$ in pyrex is sensibly constant for the time scales of interest in shock-tube work, and b) there is no apparent variation of this value with the film materials or deposition processes employed here, even at very short times.

References

- ¹ Vidal, R. J., "Model Instrumentation Techniques for Heat Transfer and Force Measurements in a Hypersonic Wind Tunnel," Rept. AD-917-A-1, WADC TN 56-315, Feb. 1956, Cornell Aerospace Lab., Buffalo, New York.
- ² Cook, W. J. and Felderman, E. J., "Reduction of Data from Thin-Film Heat-Transfer Gauges; a Concise Numerical Technique," *AIAA Journal*, Vol. 4, No. 3, March 1966, pp. 561–562.
- ³ Collins, D. J., Greif, R., and Bryson, A. E., "Measurements of the Thermal Conductivity of Helium in the Temperature Range 1600–6700°K," *International Journal of Heat and Mass Transfer*, Vol. 8, 1965, pp. 1209–1216.
- ⁴ Willeke, K., "Shock-Tube Study of the Transient Thermal Behavior of Gases at High Temperature," SUDAAR No. 375, May 1969, Stanford University, Palo Alto, Calif.

† Measured directly with a Talysurf, Taylor-Hobson surface-finish measuring unit.

‡ Obtained from Midland Silicones, Reading, England.

⁵ Busing, J. R. and Clarke, J. F., "Shock Reflection and Surface Effects in the Shock Tube," *Advances in Aerothermochemistry*, edited by I. Glassman; AGARD Proceedings, No. 12, Vol. 1, 1967, pp. 165–190.

⁶ Hanson, R. K., "Shock-Tube Measurements of Thermal Accommodation Between a Hot Gas and a Cold Solid," TR, in press, Sept. 1970, Cranfield Institute Tech., Cranfield, Beds, England.

⁷ Skinner, G. T., "Calibration of Thin Film Gage Backing Materials," *AES Journal*, Vol. 31, No. 5, May 1961, pp. 671–672.

⁸ Carslaw, H. S. and Jaeger, J. C., *Conduction of Heat in Solids*, 2nd ed., Oxford University Press, London, 1962.

Bending Stress in a Conical Shell Subjected to Thermal and Pressure Loadings

H. D. FISHER*

Sandia Laboratories, Albuquerque, N. Mex.

Introduction

THIS Note employs the perturbation method of Ref. 1 to obtain the bending stress at a clamped support of a semi-infinite conical shell subjected to a spatially uniform heat addition that is constant through the thickness and has a step function in time. As in Ref. 2, the early time response is assumed to be adequately described by a model in which heat conduction is ignored. For a specific radius to thickness ratio, numerical results reveal that the maximum bending stress at the clamped support is significantly reduced by the first-order correction to the zero-order solution, which is that for a circular, cylindrical shell. Inclusion of the second-order correction, however, has a negligible effect and thus further correction terms are not computed.

In addition, the response of the conical shell to a spatially uniform pressure with a Heaviside temporal variation is obtained by integrating the solutions derived in Ref. 1. In contrast to the thermal loading, the bending stress at the clamped support for the pressure loading is increased when the first-order correction term is included. An additional point of interest is the similarity of the plots of the dimensionless bending stress at the support vs dimensionless time for the two loadings.

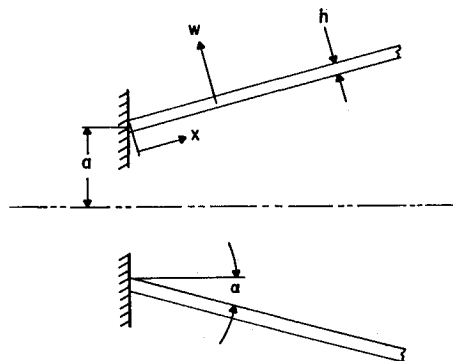


Fig. 1 Problem geometry.

Received October 26, 1970; revision received December 21, 1970. This work was supported by the U.S. Atomic Energy Commission. The author wishes to express his appreciation to Z. E. Beisinger for writing the computer program utilized in this study. He is also indebted to M. J. Forrestal for supplying the detailed calculations used in Ref. 1 and to W. A. Von Riesemann for numerical corroboration of the present study (see Ref. 4).

* Staff Member.